Available online at www.sciencedirect.com
SCIENCE DIRECT®
Journal of Nuclear Materials 329–333 (2004) 933–937
journal of nuclear materials
www.elsevier.com/locate/jnucmat

Release of helium from irradiation damage in Fe–9Cr ferritic alloy

K. Ono [a,*], K. Arakawa [a], H. Shibasaki [a], H. Kurata [b], I. Nakamichi [c], N. Yoshida [d]

[a] Department of Materials Science, Shimane University, 1060 Nishikawatsu, Matsue 690-8504, Japan
[b] Institute for Chemical Research, Kyoto University, Gokasho, Uji, Kyoto 611-0011, Japan
[c] Cryogenic Center, Hiroshima University, 1-3-1 Kagamiyama, Higahshi-Hiroshima 739-8526, Japan
[d] Research Institute for Applied Mechanics, Kyushu University, Kasuga, Fukuoka 816-8580, Japan

Abstract

Thermal desorption of helium from Fe–9Cr and pure Fe which were irradiated with 5 keV He^+ ions at 85 or 473 K have been studied by thermal desorption spectrometry (TDS) at temperatures from room temperature to 1270 K and related microstructure changes by TEM. It is found that five TDS peaks appear in Fe–9Cr specimen and these peaks are well correlated with microstructure changes. From these results, the five peaks I_{Cr}, II_{Cr}, III_{Cr}, IV_{Cr} and V_{Cr} may be attributed to release of trapped helium atoms by the break-up of vacancy–helium–self-interstitial atom complexes or very tiny loops, glide to the specimen surface or coalescence of interstitial type dislocation loops, shrinkage of dislocation loops, bubble migration to the specimen surface and α–γ phase transformation, respectively. Precipitation of Cr around the loops and bubbles in Fe–9Cr is revealed by STEM-EELS and this could shift the related TDS peaks to higher temperatures.

1. Introduction

High (9–12 wt%) Cr base steels are recognized as a leading candidate for first wall materials [1] and a number of studies have been reported and reviewed [2,3]. The excellent swelling resistance of these steels may primarily be a result of the delay in void nucleation, but is highly dependent on irradiation conditions. Hence, to obtain a general understanding of the swelling resistance, more fundamental studies performed under various irradiation conditions are required.

One of key factors which control evolution of the swelling is the interaction of irradiation induced defects with helium atoms. However, little information on the microstructure at which helium atoms are trapped and their detrapping processes in Fe–Cr ferritic alloys is available, although thermal desorption spectrometry (TDS) of helium atoms was performed for some irradiated metals [4–6]. Recently, Morishita et al. [7] studied TDS of helium from Fe and discussed a release of helium from vacancy related defects in comparison with molecular dynamics calculations. However, in that work, information on the defects that could be clarified by TEM was poor.

In the present work, thermal desorption of helium atoms from a Fe–9Cr specimen irradiated with He^+ ions and the microstructure change corresponding to the desorption spectra are investigated by TDS and TEM observation. Effects of Cr are clarified by revealing segregation of Cr around the defects using the STEM-EELS (scanning transmission electron microscopy-electron energy loss spectrometry) technique.

2. Experimental procedure

The material was a ferritic alloy which was cast from high purity starting materials supplied by

* Corresponding author.
E-mail address: onokotar@riko.shimane-u.ac.jp (K. Ono).

0022-3115/$ - see front matter © 2004 Elsevier B.V. All rights reserved.
doi:10.1016/j.jnucmat.2004.04.061

Johnson-Matthey and 99.995 at.% purity Fe supplied by Toho Zinc Co. Thin plate ($10\times10\times0.01$ mm^3) specimens for TDS and disk shaped ones (3 mm in the diameter) for TEM were pre-annealed at 1230 K for 1 h in an ultra-high vacuum furnace. The plate specimens for TDS were chemically etched before the pre-annealing. The disk shaped specimens were electrochemically polished for TEM after the pre-annealing.

The specimens for TDS were irradiated with 5 keV He^+ ions to doses of $1–2\times10^{20}$ ions/m^2 with a flux of 2.0×10^{17} ions/m^2 s at 85 or 473 K and then transferred into an ultra-high vacuum chamber for TDS, being followed by slow warming or cooling to room temperature. The specimen in the desorption chamber was linearly heated from room temperature to 1270 K at a constant heating rate of 1.5, 3 or 6 K/min by a infrared radiation system and the TDS measurement was performed using a quadrupole mass spectrometer.

Evolution of the microstructure in the specimen, which was similarly irradiated with 5 keV He^+ ions using an ion accelerator combined with a TEM [8], was observed and continuously monitored by TEM during warming-up to 1250 K.

To examine radiation induced precipitation or segregation of Cr around defects, STEM-EELS analysis was performed, using FE-TEM and Gatan-766 (Digi-PEELS). Scanning of the electron probe with a diameter of 1 nm was made on a 0.2–0.63 nm space interval and EELS spectra from L_{23} edges of Fe and Cr were measured.

3. Results and discussion

Spectra of ion currents that correspond to desorbed helium atoms from pure Fe and Fe–9Cr specimens are compared as a function of the specimen temperature in Fig. 1, where each specimen was linearly heated at a constant heating rate, following the irradiation to a dose of 2×10^{20} ions/m^2 at 85 K. The spectra for pure Fe sample show sharp peaks around 590, 700, 870, 990 and 1190 K, and these peaks are hereafter called peaks I, II, III, IV and V, respectively. Related peaks will be expressed by the same Roman numerals, classifying by suffixes. In the Fe–9Cr specimen, five similar peaks I_{Cr}, II_{Cr}, III_{Cr}, IV_{Cr} and V_{Cr} appeared around 720–760, 820, 890, 1100 and 1140 K, respectively. It is clearly shown from the figure that the alloying effect of Cr is to shift the Fe peaks to higher temperatures about 20–130 K, except the peak V_{Cr}, where the peak temperature was lowered relative to that in pure Fe.

Fig. 2 shows TDS spectra from Fe–9Cr specimens irradiated with 5 keV He^+ ions to a dose of 2.0×10^{20} ions/m^2 at 473 K. It is seen that the peak II^*_{Cr} is broad and may be overlapping with the peak I^*_{Cr}, but the other peaks III^*_{Cr}, IV^*_{Cr} and V^*_{Cr} appeared consistently in the same temperature ranges shown in Fig. 1.

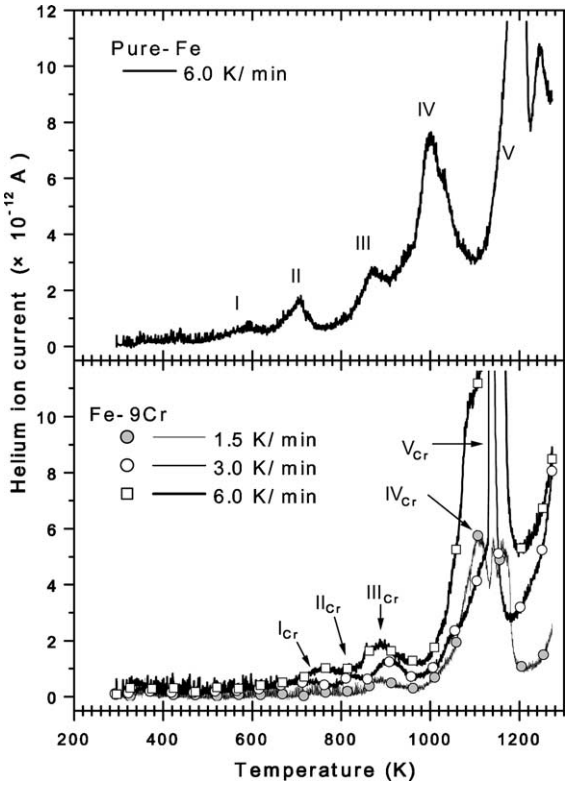

Fig. 1. Comparison of TDS spectra in Fe (upper) and Fe–9Cr (lower) specimens irradiated with 5 keV He^+ ions to a dose of 2.0×10^{20} ions/m^2 at 85 K. The linear heating rates are denoted. The peaks V and V_{Cr} are very large and the upper parts are cropped.

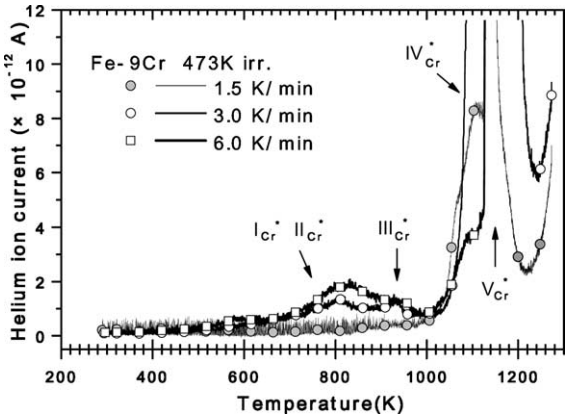

Fig. 2. TDS spectra of Fe–9Cr specimens irradiated to a dose of 2.0×10^{20} ions/m^2 at 473 K.

To examine effects of He and Cr atoms on the formation of dislocation loops in Fe–9Cr specimen, pure Fe and Fe–9Cr specimens were irradiated with 5 keV He^+ ions or 1 MeV electrons, where the dpa rate in the

electron irradiation was adjusted to the maximum one, 5×10^{-3} dpa/s, in the ion irradiation. The number density of dislocation loops formed at 473 K is compared in Fig. 3. Enhanced nucleation of loops not only by helium atoms but also by the combined effects of helium and Cr atoms is remarkable. It has been pointed out by present authors that helium–vacancy complexes play the role of nucleation sites of the interstitial loops in pure Fe [9]. This fact should affect the helium desorption peak I in pure Fe, which will be discussed below. In the case of Fe–9Cr, the high density dislocation loops shown in Fig. 3 could trap helium atoms and these helium atoms could cause the desorption peaks I_{Cr}, II_{Cr} and III_{Cr} as will be discussed below.

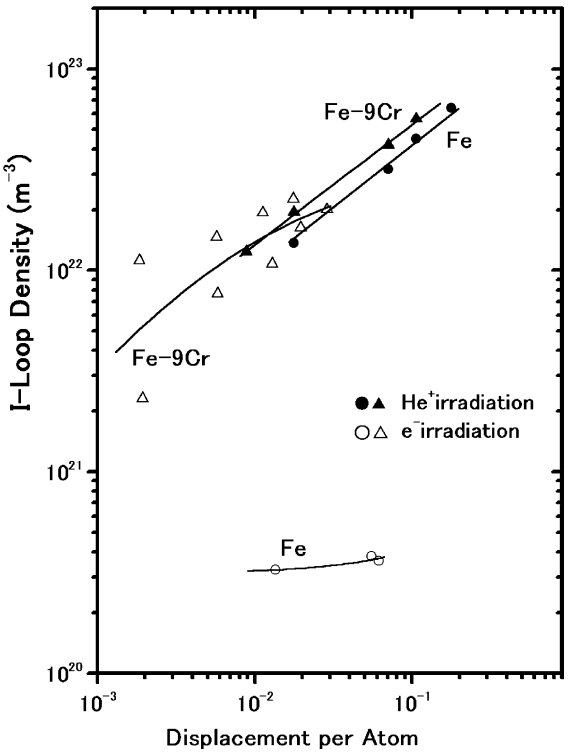

Fig. 3. Number density of dislocation loops in Fe and Fe–9Cr irradiated with 5 keV He^+ ions or 1 MeV electrons as a function of the dpa. In the ion irradiation, the loop number density and the dpa at the maximum depth distribution were adopted. The dpa rates in both irradiations were same.

The desorption spectra discussed above can be related to the microstructure change observed in detail by TEM. In the case of pure Fe, peaks I, II, III are attributed to release of trapped helium atoms by break-up of helium–vacancy–self-interstitial atom complexes or very tiny I-type loops, glide to the specimen surface or coalescence of gliding dislocation loops and shrinkage of the loops, respectively. The temperatures of the peaks II and III seem close to that of helium desorption from dislocations in deformed Fe [6]. The peaks IV and V are attributed to release of helium by migration of helium bubbles to the specimen surface and phase transformation from α to γ phase, respectively. The details will be reported elsewhere [10].

In the case of a Fe–9Cr specimen, the microstructure change by heating to higher temperatures following the irradiation with 5 keV He^+ ions at 85 K is shown in Fig. 4. As seen from the micrograph, high density dislocation loops are observed at room temperature, which almost disappear by about 900 K. By observation in more detail, it was noticed that very tiny complexes or loops disappeared around 700–770 K and the remaining loops grew. These loops started to change their configuration by gliding and coalescence around 770–850 K. The glide motion was very slow in comparison with that in pure Fe. Most of the loops disappeared at around 940 K, which could be caused by absorption of thermal vacancies [11], with the activation energy for the self-diffusion in Fe of 2.9 eV[12]. Small size bubbles (1–2 nm in diameter) became obvious in the TEM image above around 800 K and started to move above 990 K, depending on their size and shape. Some of bubbles

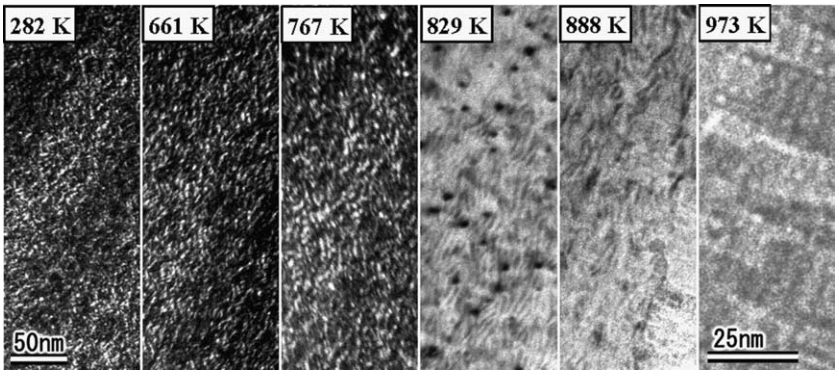

Fig. 4. Microstructure change in Fe–9Cr specimen by annealing, following irradiation with 5 keV He^+ ions to a dose of 2.0×10^{19} ions/m^2 at 85 K. The first three micrographs are dark field image and the others are bright field. The final one is higher magnification.

disappeared at the specimen surface and some coalesced. The motion profile and mobility of helium bubbles in Fe and Fe–9Cr have been reported by the present authors [13]. The phase transformation from α to γ phase takes place around 1140 K and most bubbles were swept out following a movement of the phase boundary [14].

The microstructure change shown in Fig. 4 is well correlated with the desorption spectra shown in Fig. 1. Therefore, we should be able to attribute the TDS peaks I_{Cr}, II_{Cr}, III_{Cr}, IV_{Cr} and V_{Cr} to the release of helium atoms by break-up of very tiny interstitial complexes or loops, glide to the specimen surface or glide and coalescence of dislocation loops, shrinkage of dislocation loops by absorption of thermal vacancies, bubble motion to the specimen surface and phase transformation, respectively. Lowering of the peak V_{Cr} temperature in Fe–9Cr is in good agreement with a Fe–Cr phase diagram.

Morishita et al. [7] indicated from a molecular dynamics calculation that interstitial or substitutional helium in Fe is able to move easily above room temperature, while the helium atom is strongly bound to helium–vacancy clusters. Berg et al. [15] suggested strong binding of helium atoms to edge dislocation in Fe. These calculations of the strong bindings seem to support present results. That is, the spectra I, II and III, or I_{Cr}, II_{Cr} and III_{Cr} are basically attributed to the annihilation of loop dislocation segments and the annihilation of the deep trapping sites is the easiest process for helium release at these temperatures of the peaks. Bubble migration at temperatures of peaks IV and IV_{Cr} was confirmed and should be an easier process than the helium resolution into the matrix from bubbles in Fe and Fe–9Cr.

Segregation of Cr induced by irradiation was analyzed by STEM-EELS. For helium bubbles in the Fe–9Cr alloy, Cr segregation on their surface has been revealed by present authors [13]. For dislocation loops formed by irradiation with He^+ ions in Fe–9Cr, an elemental mapping of Fe and Cr across the loop is shown in Fig. 5. The upper half of the figure is an annular dark filed (ADF) image of edge-on dislocation loops and the lower half indicates local distributions of Fe and Cr which were obtained by measurement of EELS spectra from L_{23} edges along the white line in the ADF image in 0.63 nm interval. The number of electrons in the vertical axis was calculated by subtracting the background intensity from each edge of raw spectra. From combined consideration of EELS spectra with the intensity spectra of ADF dislocation loop image, we can judge that at the position of the dislocation loop, the concentration of Fe is decreased and that of Cr is increased. The segregated Cr around the dislocation loop or bubble could retard the motion of dislocations and bubbles and shift the related desorption spectra to higher temperatures. The retardation of the bubble mobility by segregated Cr in Fe–9Cr has been clarified by the present authors [13].

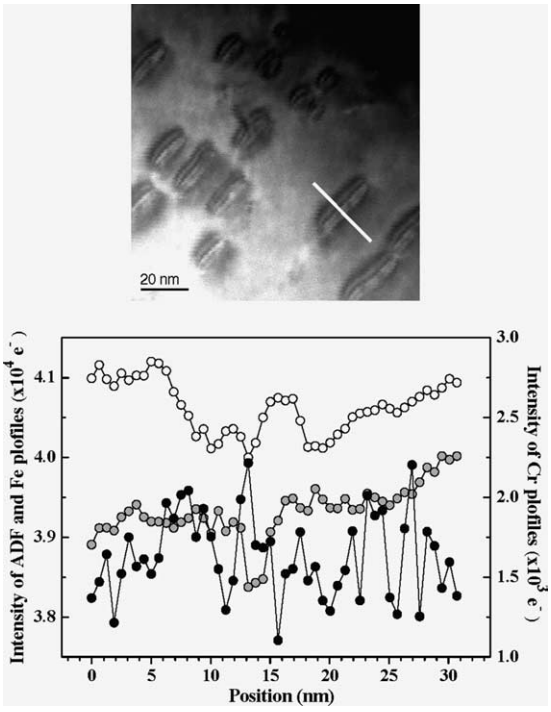

Fig. 5. The upper part is the ADF image of edge-on dislocation loops in Fe–9Cr. The lower part shows the distribution of Fe (○) and Cr (●) which were obtained by STEM-EELS analysis measured along the white line in the ADF image. For the Fe distribution, 1.8×10^4 electrons are added for easy comparison with Cr one. The intensity profile of ADF image (◯) is also shown to indicate the position of the loop.

4. Conclusions

Trapping states of helium atoms and their release from Fe–9Cr and Fe specimens which were irradiated with 5 keV He^+ ions have been examined by TDS, TEM and STEM-EELS. The important point in the present work is that TDS spectra are well correlated with the microstructure change revealed by TEM and STEM-EELS. The main conclusions are as follows:

1. TDS spectra I_{Cr}, II_{Cr} and III_{Cr} appeared at around 720–760, 820 and 890 K and these are attributed to a release of helium by break up of interstitial complexes or tiny loops, annihilation of loop dislocation segments owing to glide, coalescence and disappearance of loops by absorption of thermal vacancies, respectively.
2. The peak IV_{Cr} appeared at around 1100 K and this can be attributed to the migration of helium bubbles to the specimen surface.

3. The large peak V_{Cr} appeared at around 1140 K and can be attributed to the sweeping out of bubbles, following the movement of the α–γ phase boundary.
4. Segregation of Cr around the dislocation loops was revealed by STEM-EELS. These segregated Cr atoms could shift the spectra I_{Cr}, II_{Cr}, III_{Cr} and IV_{Cr} to higher temperatures.

References

[1] A. Kohyama, A. Hishinuma, D.S. Gell, R.L. Klueh, W. Diets, K. Ehrich, J. Nucl. Mater. 233–237 (1996) 138.
[2] F.A. Garner, M.B. Toloczko, B.H. Sencer, J. Nucl. Mater. 276 (2000) 123.
[3] R.L. Klueh, D.H. Harries, High chromium ferritic and martensitic steels for nuclear applications, ASTM stock number: MONO3, 2001.
[4] A. van Veen, in: S.E. Donnelly, J.H. Evans (Eds.), Fundamental Aspects of Inert Gases in Solids, Plenum, NY, 1991, p. 41.
[5] P. Jung, C. Liu, J. Chen, J. Nucl. Mater. 296 (2001) 165.
[6] R. Sugano, K. Morishita, H. Iwakiri, N. Yoshida, J. Nucl. Mater. 307–311 (2002) 941.
[7] K. Morishita, R. Sugano, H. Iwakiri, N. Yoshida, A. Kimura, in: S. Hanada, Z. Zhong, S.W. Nam, R.N. Wright (Eds.), Proceedings of 4th Pacific Rim International Conference on Advanced Materials and Processing, The Jpn. Inst. Met., 2001, pp. 1395, 1383.
[8] K. Arakawa, T. Tsukamoto, K. Yasuda, K. Ono, J. Electron Microsc. 48 (1999) 399.
[9] K. Arakawa, R. Imamura, K. Ohota, K. Ono, J. Appl. Phys. 89 (2001) 4752.
[10] K. Ono, K. Arakawa, H. Shibasaki, submitted for publication.
[11] P.S. Dobson, P.J. Goodhew, R.E. Smallman, Philos. Mag. 13 (1967) 9.
[12] A. Seeger, Phys. Stat. Sol. (a) 167 (1998) 289.
[13] K. Ono, K. Arakawa, K. Hojou, J. Nucl. Mater. 307–311 (2002) 1507.
[14] K. Ono, K. Arakawa, H. Shibasaki, submitted for publication.
[15] F.v.d. Berg, W. van Heugten, L.M. Caspers, A. van Veen, Solid State Commun. 24 (1977) 193, 27 (1978) 665.